

## Numerical analysis of the Higgs mass triviality bound

URS M. HELLER<sup>a</sup>, MARKUS KLOMFASS<sup>b</sup>,  
HERBERT NEUBERGER<sup>c</sup>,  
PAVLOS VRANAS<sup>a</sup>

<sup>a</sup> *Supercomputer Computations Research Institute*

*The Florida State University*

*Tallahassee, FL 32306*

<sup>b</sup> *Department of Physics*

*Columbia University*

*New York, NY 10027*

<sup>c</sup> *Department of Physics and Astronomy*

*Rutgers University*

*Piscataway, NJ 08855-0849*

ABSTRACT: Previous large  $N$  calculations are combined with numerical work at  $N = 4$  to show that the Minimal Standard Model will describe physics to an accuracy of a few percent up to energies of the order 2 to 4 times the Higgs mass,  $M_H$ , only if  $M_H \leq 710 \pm 60 \text{ GeV}$ . This bound is the result of a systematic search in the space of dimension six operators and is expected to hold in the *continuum*. Given that studying the scalar sector in isolation is already an approximation, we believe that our result is sufficiently accurate and that further refinements would be of progressively diminishing interest to particle physics.

## 1. INTRODUCTION AND CONCLUSION.

Our goal is to obtain an estimate for the triviality bound on the Higgs mass in the minimal standard model. Much work has preceded this paper (for examples consult [1,2,3,4,5,6] and the review [7]). We build on these results and generalize them. Specifically, we deal more systematically with the quantitative uncertainty resulting from the arbitrariness of the coefficients of higher dimensional operators in the scalar sector [8]. By doing this we aim to obtain a number that is meaningful beyond *lattice* field theory and directly relevant to particle physics.

The overall framework of the approach has been reviewed before (e.g. [8]) and will not be repeated here. Its main simplifying feature is to treat the scalar sector of the minimal standard model in isolation. When considering further efforts in this framework the potential impact on particle physics should be evaluated against the accuracy of neglecting other interactions, e.g. with the top quark. We believe that our result is reliable to a reasonable degree, given that the whole framework is an approximation, and we feel that further refinements would be of progressively diminishing interest to particle physics\*.

Our result is that the minimal standard model will describe physics to an accuracy of a few percent up to energies of the order 2 to 4 times the Higgs mass,  $M_H$ , only if  $M_H \leq 710 \pm 60 \text{ GeV}$ . The two major assumptions made are that ignoring all couplings but the scalar self-coupling is a good approximation and that any higher energy theory into which the standard model is embedded will not conspire to eliminate all dimension six scalar field operators in the low energy effective action. The number we obtain is not surprising because of its closeness to tree level bounds [1,3]; what has been achieved is to finally show that in any reasonable situation higher orders in perturbation theory cannot change it substantially although quite strong scalar self-interactions are possible.

In the sequel we shall rely quite heavily on [9] but we also try to make the paper accessible to readers who are not familiar with [9]. Our basic strategy was to first use  $\frac{1}{N}$  expansion techniques in the generalization of the  $O(4)$  symmetric scalar sector to  $O(N)$  to obtain an analytical non-perturbative estimate for the bound and then follow up with Monte Carlo simulations at the physical value  $N = 4$ . In the next section we summarize needed information at  $N = \infty$  and add some new results in this limit. The following section presents our numerical work with some emphasis on the checks that were made to ascertain control over systematic errors. The last section explains our main conclusion. Appendix A gives a few more details on the new large  $N$  results, and finally in appendix B we collect the numbers obtained from our simulations in several tables matching the graphs shown in the main text.

---

\* An exception would be further investigations of the Higgs width on the lattice.

Our notational conventions are: The Higgs mass in physical units ( $GeV$ ), defined as the real part of the resonance pole, is denoted by  $M_H$  and the width by  $\Gamma_H$ . The same quantities in lattice units are denoted by lower case letters,  $m_H$  and  $\gamma_H$ . The matrix element of conventionally normalized currents of broken symmetries between the vacuum and single Goldstone boson states (referred to as pions,  $\pi$ ) is denoted by  $F$  in physical units and by  $f$  in lattice units. The scalar self-coupling is defined by:

$$g = \frac{3M_H^2}{F^2} . \quad (1.1)$$

In the  $N = \infty$  section everything is written in terms of the above  $N = 4$  notation. We use  $\Lambda$  to denote a generic cutoff.

Most of our work is on the  $F_4$  lattice which can be thought of as embedded in a hypercubic lattice from which odd sites (i.e. sites whose integer coordinates add up to an odd sum) have been removed. The lattice spacing of the hypercubic lattice is  $a$ . It is set to unity when  $m_H$ ,  $\gamma_H$  and  $f$  are used. The  $F_4$  lattice is always fully symmetric having, when finite,  $L$  sites in each principal axis direction so that the total number of sites is  $L^4$ . Usually,  $x, x', x''$  denote sites,  $\langle x, x' \rangle, l, l'$  links,  $\ll x, x' \gg$  next-nearest-neighboring pairs,  $\langle l, l' \rangle$  pairs of links, and the field is constrained by  $\vec{\Phi}^2(x) = 1$ .

## 2. RESULTS AT LARGE $N$ .

Here we summarize the large  $N$  results of [9] relevant to our numerical work. They contain predictions that can be directly compared to  $N = 4$  Monte Carlo data and evaluations of observable cutoff effects on  $\pi - \pi$  scattering. The dependence of the bound on the magnitude of the observable cutoff effects is relatively insensitive: a change by a factor of 3 induces a variation of 50  $GeV$  in the bound in the worst case. Thus, we do not worry about  $\frac{1}{N}$  corrections to the cutoff effects. Cutoff effects could also be calculated in perturbation theory but we have argued (see Appendix B of [9]) that the  $\frac{1}{N}$  computation is probably more reliable. Hence we use the  $\frac{1}{N}$  results here.

### 2.1. Relaxing the bound.

The naïve expectation that heavier Higgs masses are obtained when the bare scalar self-coupling is increased is upheld by nonperturbative calculations. The search for the bound can therefore be restricted to nonlinear actions.

Among the nonlinear actions the bound is further increased by reducing as much as possible the attraction between low momentum pions in the  $I = J = 0$  channel. Given

a bare action the approximate combination of parameters achieving this is identified as follows. Expand in slowly varying fields and use a field redefinition to bring the action, including terms up to fourth order in the momenta, to the form

$$S_c = \int_x \left[ \frac{1}{2} \vec{\phi} (-\partial^2) \vec{\phi} - \frac{b_1}{2N} (\partial_\mu \vec{\phi} \cdot \partial_\mu \vec{\phi})^2 - \frac{b_2}{2N} (\partial_\mu \vec{\phi} \cdot \partial_\nu \vec{\phi} - \frac{1}{4} \delta_{\mu,\nu} \partial_\sigma \vec{\phi} \cdot \partial_\sigma \vec{\phi})^2 \right] . \quad (2.1.1)$$

At  $N = \infty$   $b_2$  has no effect and the bound depends monotonically on  $b_1$ , increasing with decreasing  $b_1$ . Overall stability of the homogeneous broken phase restricts the range of  $b_1$ . For example on the  $F_4$  lattice, at the optimal value of  $b_1$  the bound is increased by about 100 *GeV* relative to the simplest non linear action.

The rule in the above paragraph does not lead to an exactly universal bound. Different bare actions that give the same effective parameter  $b_1$  can give somewhat different bounds because the dependence of physical observables on the bare action is highly nonlinear. For example, at the optimal  $b_1$  value, Pauli–Villars regularizations lead to bounds higher by about 100 *GeV* than some lattice regularizations. This difference between the lattice and Pauli–Villars can be traced to the way the free massless inverse Euclidean propagator departs from the  $O(p^2)$  behavior at low momenta. For Pauli–Villars it bends upwards to enforce the needed suppression of higher modes in the functional integral, while on the lattice it typically bends downwards to reflect the eventual compactification of momentum space.

Because we desire to preserve Lorentz invariance to order  $1/\Lambda^2$  we use the  $F_4$  lattice and, on the basis of the above observations, there are three stages of investigation. The first stage is to investigate the naïve nearest–neighbor model. This should be viewed as the generic lattice case where no special effort to increase the bound is made. Since this case has been investigated thoroughly in [5] we can proceed to more complicated actions with well tested methods of analysis. The next stage is to write down the simplest action that has a tunable parameter  $b_1$ . The last stage is to add a term to eliminate the “wrong sign” order  $p^4$  term in the free nearest–neighbor propagator, amounting to Symanzik improvement of

the large  $N$  pion propagator. The three  $F_4$  actions, investigated at large  $N$ , are given by

$$\begin{aligned}
S'_1 &= -2N\beta_0 \sum_{\langle x, x' \rangle} \vec{\Phi}(x) \cdot \vec{\Phi}(x') \\
S'_2 &= S'_1 - \frac{N\beta_2}{48} \sum_x \left[ \sum_{\substack{l \cap x \neq \emptyset \\ l = \langle x, x' \rangle}} \vec{\Phi}(x) \cdot \vec{\Phi}(x') \right]^2 \\
S'_3 &= -N\beta_0 \sum_x \left[ 2 \sum_{x' \text{ n.n. to } x} \vec{\Phi}(x) \cdot \vec{\Phi}(x') - \frac{1}{2} \sum_{x'' \text{ n.n.n. to } x} \vec{\Phi}(x) \cdot \vec{\Phi}(x'') \right] \\
&\quad - \frac{N\beta_2}{72} \sum_x \left[ 2 \sum_{x' \text{ n.n. to } x} \vec{\Phi}(x) \cdot \vec{\Phi}(x') - \frac{1}{2} \sum_{x'' \text{ n.n.n. to } x} \vec{\Phi}(x) \cdot \vec{\Phi}(x'') \right]^2 .
\end{aligned} \tag{2.1.2}$$

These actions were chosen because they have relatively simple large  $N$  limits and permit a simultaneous study of both  $F_4$  and hypercubic lattices. In each case, at constant  $\beta_2$ ,  $\beta_0$  is varied tracing out a line in parameter space approaching a critical point from the broken phase. This line can also be parameterized by  $m_H$  or  $g$ . For actions  $S'_2$  and  $S'_3$ ,  $\beta_2$  is chosen so that on this line the bound on  $M_H$  is expected to be largest. A simulation produces a graph showing  $\frac{m_H}{f}$  as a function of  $m_H$  along this line. The y-axis is turned into an axis for  $M_H$  by  $M_H = \frac{m_H}{f} \times 246 \text{ GeV}$ . The large  $N$  predictions for these graphs are shown in Figure 2.1. Since action  $S'_3$  was not treated in [9] we include a brief account in appendix A.

## 2.2. Cutoff Effects.

At  $N = \infty$  the cutoff effects to order  $1/\Lambda^2$  on the Higgs width and  $\pi - \pi$  scattering are parameterizable by:

$$S_{eff} = S_R(g) + c \exp[-96\pi^2/g] \mathcal{O}(g) . \tag{2.2.1}$$

$S_R$  contains only universal information and so does  $\mathcal{O}$ . All the non-universal information is in the  $g$  independent parameter  $c$ . The form of  $S_{eff}$  reflects the factorization of cutoff effects into a universal  $g$  dependent function and a  $g$  independent non-universal amplitude. The bound is increased by first varying the non-universal part so that  $c$  decreases at constant  $g$  and then going along the selected line to higher  $g$ .

$\bar{\delta}_{|A|^2}$  denotes the fractional deviation of the square of the  $\pi^a - \pi^a$  ( $a$  identifies one of the  $N - 1$  directions transverse to the order parameter in internal space) scattering amplitude at 90 degrees in the CM frame at energy  $W$  from its large  $N$  universal value. A plot of  $\bar{\delta}_{|A|^2}$

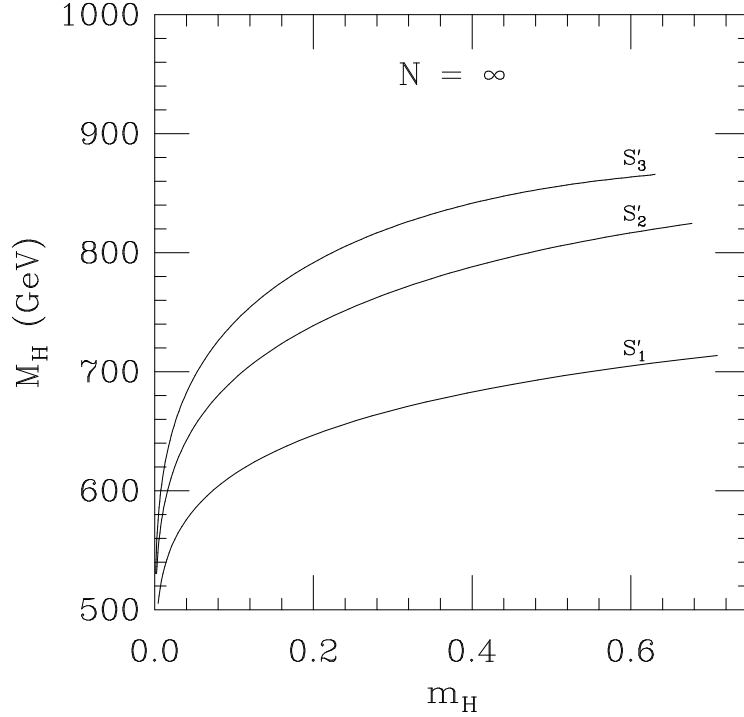


**Figure 2.1** The Higgs mass  $M_H = \frac{m_H}{f} \times 246 \text{ GeV}$  in physical units vs. the Higgs mass  $m_H$  in lattice units for the three actions, eq. (2.1.2).

as a function of  $M_H(m_H)$  for the three actions is presented in Figure 2.2. If one considers only the magnitude of cutoff effects as a function of  $m_H = \frac{M_H}{\Lambda}$ , one might conclude that the bound obtained with action  $S'_1$  would be larger than the bound obtained with  $S'_2$ . This conclusion proves to be wrong when the mass in physical units is considered. The values of  $M_H$  in  $\text{GeV}$ , determined from  $M_H = \frac{m_H}{f} \times 246 \text{ GeV}$ , are put on three horizontal lines in Figure 2.2 at  $\bar{\delta}_{|A|^2} = 0.005, 0.01, 0.02$ . At large  $N$  the bound increases when going from  $S'_1$  to  $S'_2$  and then to  $S'_3$  by a little over 10% at each step. For example, for  $\bar{\delta}_{|A|^2} = .01$  we get bounds on  $M_H$  of 680, 764, 863  $\text{GeV}$  for  $S'_1, S'_2$  and  $S'_3$  respectively.

### 2.3. Width.

The width  $\Gamma_H$  is important for phenomenology and for lattice work (see sect. 3.4). With massless pions perturbation theory seriously underestimates  $\Gamma_H$  when  $M_H$  is large [9].

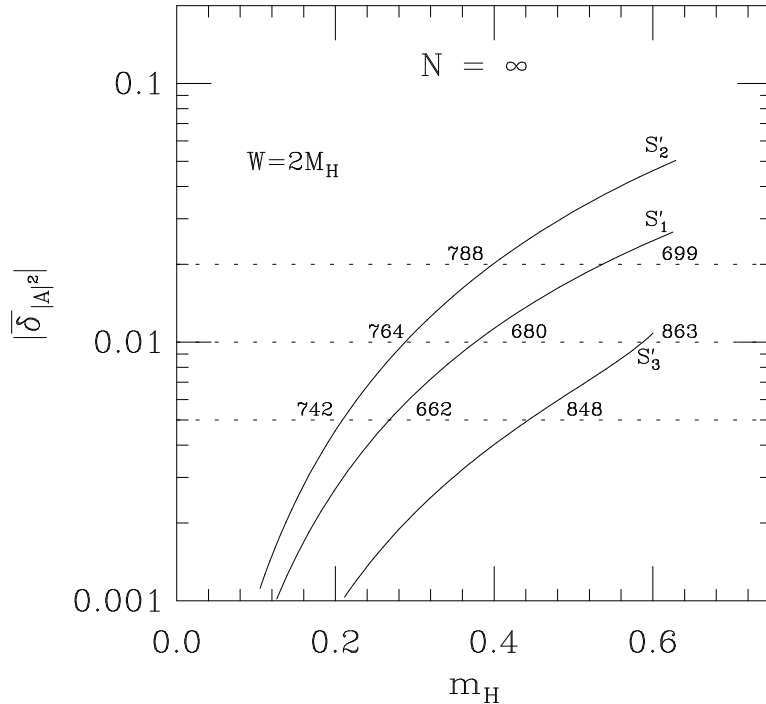


**Figure 2.2** Leading order cutoff effects in the invariant  $\pi - \pi$  scattering amplitude at  $90^\circ$  at center of mass energy  $W = 2M_H$  vs. the Higgs mass in lattice units for the three actions. The values of  $M_H$  in  $GeV$  determined from  $M_H = \frac{m_H}{f} \times 246 \text{ GeV}$  are put on the three horizontal lines at  $\bar{\delta}_{|A|^2} = 0.005, 0.01, 0.02$ .

It would therefore be desirable to determine the width non-perturbatively. Up to date the only methods known for measuring the width within a numerical simulation require a non-zero pion mass [10]. To study the effects of a non-zero pion mass we computed the width in this case at large  $N$ . The mass for the pions was induced by an external magnetic field that breaks the symmetry explicitly [11]. Because the cutoff effects on the width are very small we show in Figure 2.3 only the universal part and compare it to the leading order perturbative values. Shown are the two results for  $M_\pi = 0, 100, 200,$  and  $300 \text{ GeV}$ .

We see that the deviations from perturbation theory decrease when the pion mass increases. Therefore to detect nonperturbative effects on the width at  $N = 4$  one would have to deal either with the massless case directly or, at least, with quite light pions, say  $M_\pi \lesssim \frac{1}{6}M_H$ . This is one point we believe deserves further study.

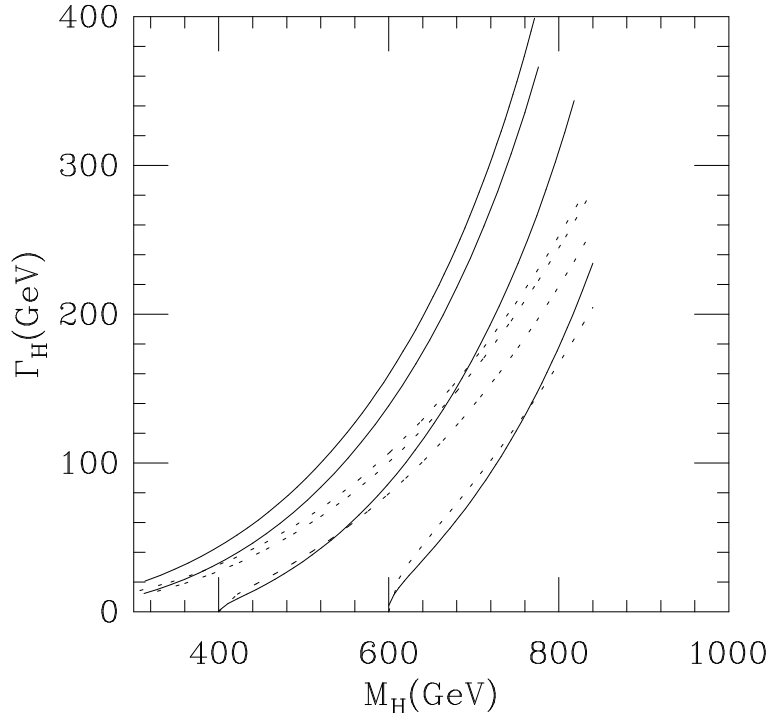


**Figure 2.3** The universal part of the width vs.  $M_H$ . The solid line displays the large  $N$  result scaled to  $N = 4$  and the dotted line shows the leading order term in perturbation theory. From left to right the lines correspond to pion masses  $M_\pi = 0, 100, 200,$  and  $300 \text{ GeV}$ .

### 3. THE PHYSICAL CASE $N = 4$ .

The primary aim of the numerical work is to produce at  $N = 4$  the analogues of the graphs in Figure 2.1. The actions simulated are slightly different than those investigated at large  $N$ . Firstly, the factors  $N$  accompanying the couplings in (2.1.2) are omitted. Secondly, we take advantage of the fact that on the  $F_4$  lattice, unlike on the hypercubic lattice, the simplest action with a tunable parameter  $b_1$  can be constructed in a way that maintains the nearest-neighbor character of the action. This is done by coupling fields sited at the vertices of elementary bond-triangles. Finally we add a term to eliminate the “wrong sign” order  $p^4$  term in the free nearest-neighbor propagator, leaving, unlike in  $S'_3$ , the term with the tunable  $b_1$  coupling unchanged. This new term couples next-



nearest-neighbors and amounts to tree level Symanzik improvement.\* The three  $F_4$  actions simulated (with  $S_i$  having the same expansion in slowly varying fields as  $S'_i$  investigated at large  $N$ ) are

$$\begin{aligned}
S_1 &= -2\beta_0 \sum_{\langle x, x' \rangle} \vec{\Phi}(x) \cdot \vec{\Phi}(x') \\
S_2 &= S_1 - \frac{\beta_2}{8} \sum_x \sum_{\substack{\langle ll' \rangle \\ l, l' \cap x \neq \emptyset, l \cap x' \neq \emptyset, l' \cap x'' \neq \emptyset \\ x, x', x'' \text{ all n.n.}}} \left[ \left( \vec{\Phi}(x) \cdot \vec{\Phi}(x') \right) \left( \vec{\Phi}(x) \cdot \vec{\Phi}(x'') \right) \right] \\
S_3 &= -2(2\beta_0 + \beta_2) \sum_{\langle x, x' \rangle} \vec{\Phi}(x) \cdot \vec{\Phi}(x') + (\beta_0 + \beta_2) \sum_{\ll x, x' \gg} \vec{\Phi}(x) \cdot \vec{\Phi}(x') \\
&\quad - \frac{\beta_2}{8} \sum_x \sum_{\substack{\langle ll' \rangle \\ l, l' \cap x \neq \emptyset, l \cap x' \neq \emptyset, l' \cap x'' \neq \emptyset \\ x, x', x'' \text{ all n.n.}}} \left[ \left( \vec{\Phi}(x) \cdot \vec{\Phi}(x') \right) \left( \vec{\Phi}(x) \cdot \vec{\Phi}(x'') \right) \right] .
\end{aligned} \tag{3.1}$$

The data for action  $S_1$  can be found in [5]. Preliminary data for action  $S_2$  were presented in [8,12] and references therein. Our main task is to finalize the results for action  $S_2$  and carry out some new measurements for action  $S_3$ .

Each action is investigated in two main steps. First, the phase diagram is established; next, a particular line is chosen in the broken phase, which for actions  $S_2$  and  $S_3$ , amounts to picking a value for  $\beta_2$ . On this line we make several measurements at different values of  $\beta_0$  approaching the critical point  $\beta_{0c}(\beta_2)$ . We chose  $\beta_2$  based on the large  $N$  criteria and on the measured structure of the phase diagram. We may therefore be missing the “best” action, but, from our experience at large  $N$ , we expect at most a 20 – 30  $GeV$  additional increase in the bound. Because we object to excessive fine-tuning and since one may view what we are doing already as some amount of fine tuning, the 20 – 30  $GeV$  might go in either direction and represents the systematic uncertainty that we assign to the question of fine tuning.

### 3.1. Methods in General.

We follow closely the approach of [5]. We use a Metropolis algorithm to map out the phase diagram and a single cluster spin reflection algorithm, tested against the Metropolis algorithm, for the actual measurements. Typically we use 10,000 – 100,000 lattice passes, depending on lattice size and couplings, and simulate systems of increasing sizes with even

---

\* On the hypercubic lattice tree level improvement of the simplest action may also help reduce Lorentz violation effects at order  $1/\Lambda^2$  and was investigated in [6].

$L$  (to avoid frustration effects),  $L = 6, \dots, 16$ . The spin update speeds on a single processor CRAY Y-MP are about  $20 \frac{\mu\text{sec}}{\text{site}}$  for action  $S_1$ ,  $50 \frac{\mu\text{sec}}{\text{site}}$  for  $S_2$  and  $55 \frac{\mu\text{sec}}{\text{site}}$  for  $S_3$ .

The total computer time invested is 400 *hrs* for action  $S_1$ , 500 *hrs* for  $S_2$  and 400 *hrs* for  $S_3$ . The approximate constancy of the total amount of time spent for each action, in spite of the significant increase in complexity indicated by the rise of time per spin update, reflects the diminishing need for checks as confidence in the numerical methods builds up. The total amount of time spent, approximately 1300 *hrs*, is quite modest and shows that careful preparation, continuous support by analytical work and an incremental approach pay off.

Statistical errors are always treated by the Jackknife method and in least  $\chi^2$ -fits correlations between measurements are taken into account.

### 3.2. Phase Diagrams.

For actions  $S_2$  and  $S_3$  we determine critical points  $\beta_{0c}(\beta_2)$  at several fixed  $\beta_2$ 's using Binder cumulants of the magnetization  $\mathcal{M} = \frac{\sum_x \vec{\Phi}(x)}{L^4}$ . The critical points are obtained from the intersection points of the Binder cumulant graphs for different volumes, produced by reweighting and patching [13] the measurements from several couplings  $\beta_0$ . The results are shown in Figures 3.1 and 3.2 and the actual numbers are listed in Tables 1 and 2. They compare well with our large  $N$  results which were helpful in deciding where to scan in the first place. At large  $N$  the critical lines are straight, a feature that seems to persist at  $N = 4$ .

Based on our large  $N$  work we know that we want extremal values of  $\beta_2$  [9]. By this we mean the most negative value of  $\beta_2$  for which the leading term in the long wavelength expansion, eq. (2.1.1), still has the usual ferromagnetic sign on the critical line (*i.e.*  $\beta_{0c} + \beta_2 \gtrsim 0$ ). We therefore select  $\beta_2 = -0.11$  for actions  $S_2$  and  $S_3$ . The critical points at  $\beta_2 = -0.11$  are  $\beta_{0c} = 0.1118(3)$  and  $\beta_{0c} = 0.1113(2)$  respectively. The specific points we choose to study in detail are shown in Figures 3.1 and 3.2.

### 3.3. Coupling Constant.

To obtain the coupling constant  $g$ , eq. (1.1), we need  $f$  and  $m_H$ .  $f$  is obtained from measuring the magnetization,  $\mathcal{M}$ , and the pion wave function renormalization constant,  $Z_\pi$ , defined from the residue of the pole at zero momentum in the pion-pion propagator. The pion field,  $\vec{\pi}$ , is defined as the component of  $\vec{\Phi}$  transverse to  $\mathcal{M}$ , and for low momenta we have  $\langle |\vec{\pi}(p)|^2 \rangle = \frac{Z_\pi^2}{p^2} + \text{regular terms}$ . The magnetization is obtained by extrapolating

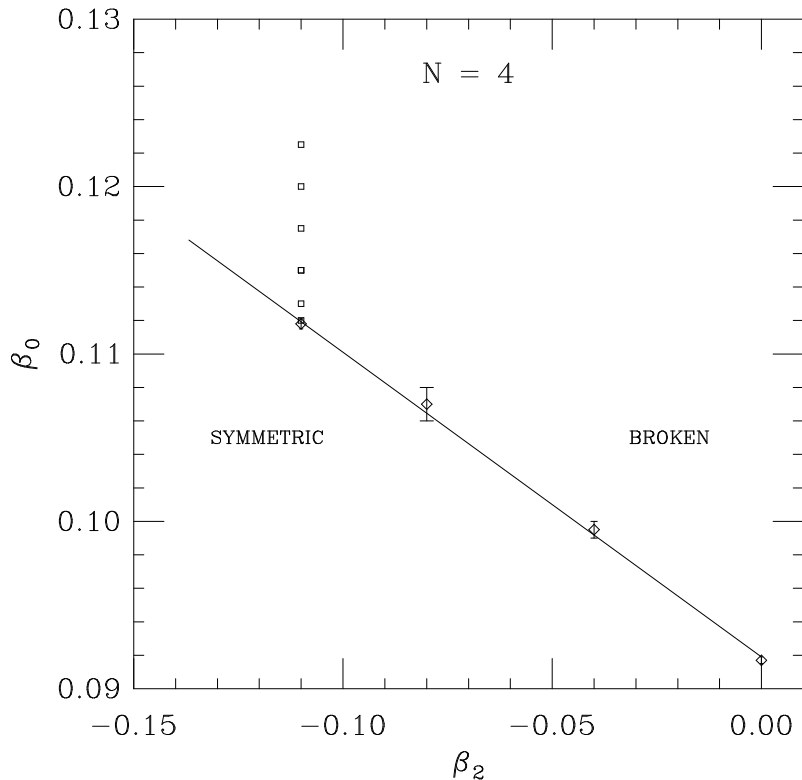


**Figure 3.1** Phase diagram for action  $S_2$ . The solid line is a least square straight line fit to the data that are denoted by diamonds. The squares indicate the points where we made simulations to determine  $m_H$  and  $f_\pi$ . They all lie on the vertical line  $\beta_2 = -0.11$ .

to  $L = \infty$  the quantities  $\langle \mathcal{M}^2 \rangle_L$  with an  $O(1/L^2)$  correction, using the methods in [14].  $f$  is then obtained from  $f = \mathcal{M}/Z_\pi$ . This method is safe and the reliability of the numbers one obtains for  $f$  is high for our purposes. The error never exceeds 1.5% in the region of higher Higgs masses which we are interested in. The estimate of  $f$  by analytical methods [3] and [15] has an error of order 5% in the same region; thus  $f$  is better determined by Monte Carlo. This is due mainly to the good theoretical control one has over finite volume effects [5,6,14]. Unfortunately, for the determination of  $m_H$  we are not so lucky.

To obtain  $m_H$  we measure the correlations of zero total three-momentum sigma states and low relative momentum two-pion states at different time separations. The sigma field,  $\sigma$ , is defined as the component of  $\vec{\Phi}$  parallel to  $\mathcal{M}$ .  $m_H$  is the energy of one of the lightest states created by superpositions of the  $\sigma$  field and two-pion composite operators at zero total three-momentum and is obtained from the eigenvalues of the measured time correlation matrix. The evaluation of  $m_H$  is not as clean as that of  $f$  and the next

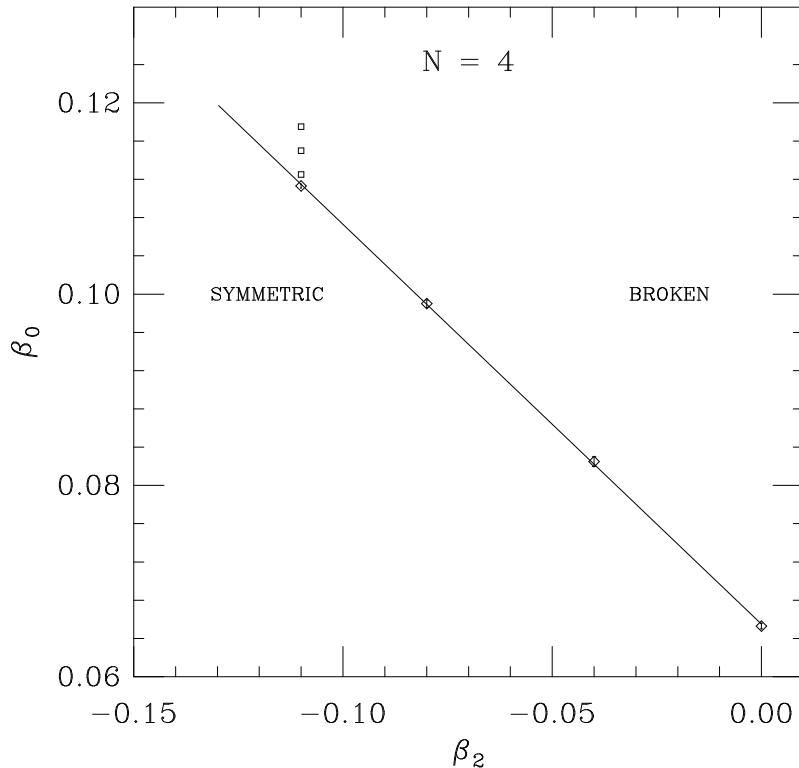


**Figure 3.2** Same as Figure 3.1 but for action  $S_3$ .

subsection discusses the determination of the numbers in greater detail.

The main result of this paper is in Figure 3.3 which shows  $M_H = 246\sqrt{g/3}$  GeV as a function of  $m_H$  for all three actions. The actual numbers are given in Tables 3, 4 and 5. One clearly sees the progressive increase of the bound. A glance at Figure 2.2 shows that in all cases the cutoff effects on the pion-pion scattering are below a few percent even at the maximal  $M_H$  of each curve. Thus we can take the largest of these maxima as our bound. The ordering of the points and their relative positions are in agreement with Figure 2.1, while the differences in overall scale, reflecting the difference between  $N = \infty$  and  $N = 4$ , come out as expected [9].

### 3.4. More about mass determination.

The main source of systematic errors is in the evaluation of  $m_H$ . In an infinite volume the Higgs particle would decay into two pions and extracting  $m_H$  from the fall-off of the  $\sigma$ - $\sigma$  correlation function would yield nonsense. In a finite volume the decay is prohibited

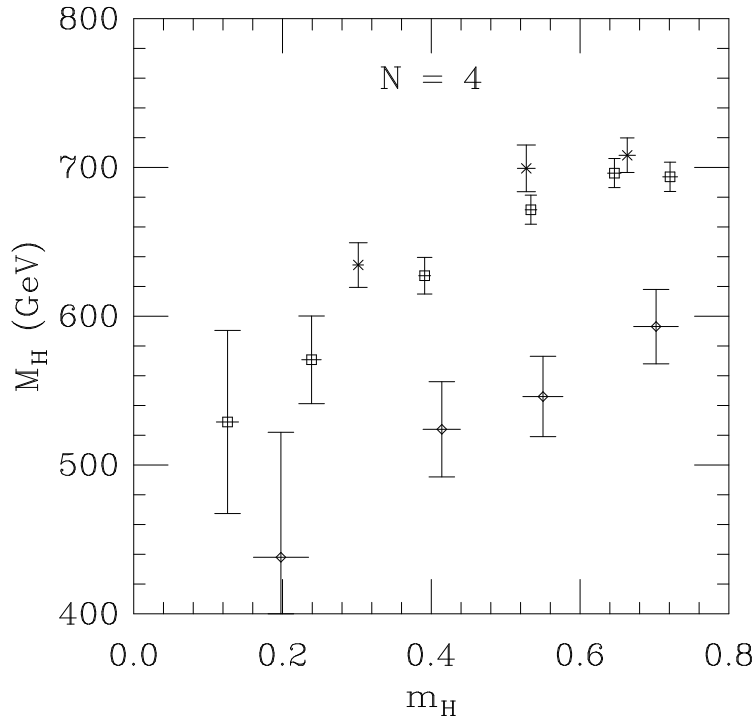


**Figure 3.3** The Higgs mass  $M_H = \frac{m_H}{f} \times 246 \text{ GeV}$  in physical units vs. the Higgs mass  $m_H$  in lattice units from the numerical simulations. The diamonds correspond to action  $S_1$  [5], the squares to action  $S_2$  and the crosses to action  $S_3$ .

or severely restricted by the rather large minimal amount of energy even the softest pions have due to momentum quantization. This makes the measurement possible but leaves one with the difficult task of estimating the accuracy of the so determined real part of the resonance pole.

In [5] we dealt with action  $S_1$ . As a check of the results obtained in the broken phase we also measured the coupling  $g$  in the symmetric phase (as defined from the zero four-momentum four-point correlation) and used perturbation theory to predict  $g$  in the broken phase. This method is free of finite width contamination and gave results consistent with the broken phase analysis. However, the determination of the coupling in the symmetric phase had a large statistical error. This problem has been eliminated by one of us [15] who carried out a complete analysis modeled on the work of [3]. The numbers of [5] survive this test reasonably. Of course, the analytical method suffers from systematic errors of a different type. It is difficult to know how much of the discrepancies at larger mass

values in the broken phase between the analytical and the Monte Carlo results are due to either approach. Still, the comparison gives a worst-case scenario for the systematics in both cases, since the methods are so different that systematics are unlikely to conspire to work in the same direction. Indeed, while the discrepancies on the  $F_4$  lattice and on the hypercubic lattice [6] are roughly of similar magnitude, the sign is opposite. We cannot be very precise, but the general conclusion we draw is that for  $\frac{m_H}{f}$  as a function of  $m_H$  the overall systematic error in the Monte Carlo results cannot exceed a few percent for the highest Higgs masses measured.

For  $S_2$  and  $S_3$  an analysis similar to [15] would be very demanding and has not been carried out. In [5] and for the lighter Higgs masses of actions  $S_2$  and  $S_3$  the Higgs mass was extracted using only the  $\sigma$  field correlation function. Since now, for the larger masses, the width is suspected to be larger some additional checks are needed. The most direct test is to write down reasonable operators that would create predominantly two pion states and check for mixing effects. We did this for action  $S_1$  at  $\beta_0 = 0.10$ , the coupling from which the bound quoted in [5] was extracted, and also for actions  $S_2$  and  $S_3$  at the couplings where we extract the bound. The large  $N$  results of section 2.3 show that more ambitious attempts to actually measure the width on the lattice by making the pions massive [11] may not be directly relevant to the massless case.

The mass is now estimated by measuring the correlation matrix  $\mathcal{C}(t)$

$$\mathcal{C}_{ij}(t) = \langle \mathcal{O}_i(t) \mathcal{O}_j(0) \rangle - \langle \mathcal{O}_i(t) \rangle \langle \mathcal{O}_j(0) \rangle$$

between several operators,  $\mathcal{O}_i$ , described in the previous subsection, evaluated on two time slices separated by  $t$  lattice spacings. The eigenvalues are determined by diagonalizing  $\mathcal{C}(t_0)^{-1/2} \mathcal{C}(t) \mathcal{C}(t_0)^{-1/2}$  as in [16] with  $t_0 = 1$  except for the largest lattice with action  $S_1$  where  $t_0 = 0$  was used. After some trials it was decided to diagonalize a  $3 \times 3$  matrix. For each lattice size we evaluate the lowest eigenvalue with this method. We also compute a “trial mass” from the  $\sigma$  field correlation function alone. When the two numbers are different within errors we expect to have some level repulsion between the two lowest eigenvalues. We then identify the eigenvalue closer to the free two pion energy as the energy of the two pion state and the other as the resonance energy. To approximately correct for the repulsion we adjust the resonance energy by the amount that the two pion energy differs from its free value. This technique should eliminate leading  $1/L$  corrections when they are significant numerically. The so obtained Higgs masses are extrapolated to  $L = \infty$  by assuming an  $\frac{1}{L^2}$  behavior. The quality of these fits is acceptable but the motivation for the method of analysis is somewhat empirical and therefore we allow for an order 3% systematic error in the mass determination.

The low lying spectrum for selected high mass values for each action are shown in Figures 3.4, 3.5 and 3.6 with the actual numbers given in Tables 6, 7 and 8. The new

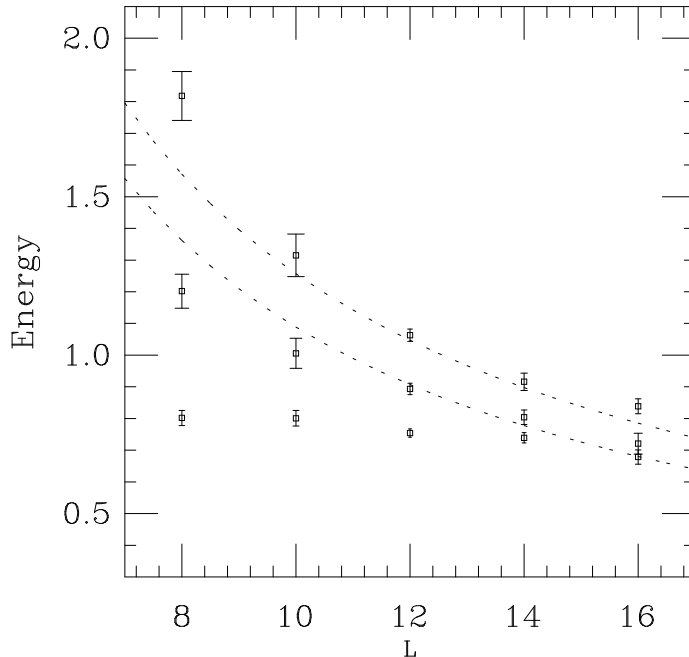


**Figure 3.4** The low lying spectrum for action  $S_1$  for various lattice sizes as measured in a numerical simulation at  $\beta_0 = 0.10$ . The dotted lines correspond to the two lowest energies of two free pions.

method of analysis confirms that the older results for action  $S_1$  are acceptable, which in turn increases our confidence when the method is applied to actions  $S_2$  and  $S_3$ . We see no indications for strong mixing because the largest level repulsions observed are small compared to the eigenvalues themselves. The two-pion states have a spectrum well described by the lattice free particle dispersion and show only small amounts of sensitivity to the resonance. Taking into account statistical errors we settle on an error estimate on the mass determinations of 5%. This results in an error of about 6% on the determination of the physical  $M_H$ .

#### 4. MAIN RESULT.

A realistic and not overly conservative value for the Higgs mass triviality bound is  $710 \text{ GeV}$ . At  $710 \text{ GeV}$  the Higgs particle is expected to have a width of about  $210 \text{ GeV}$

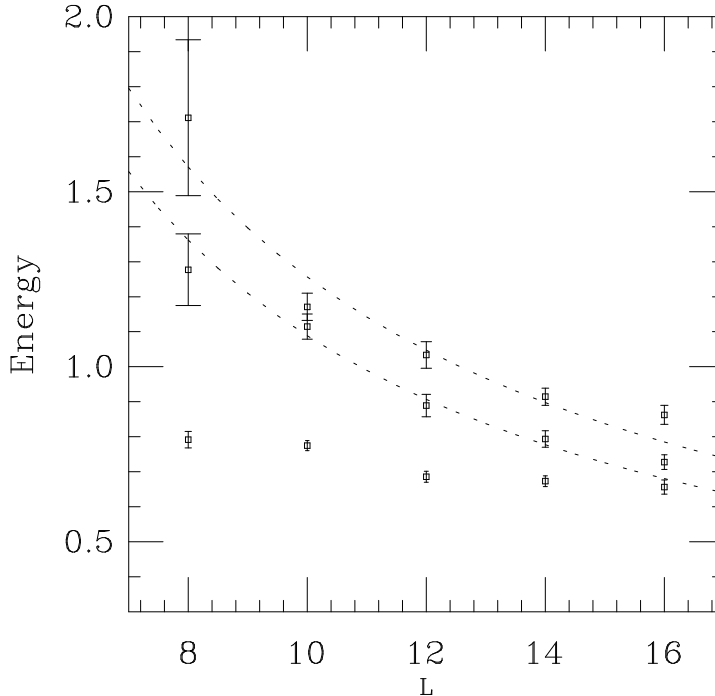


**Figure 3.5** Same as Figure 3.4 but for action  $S_2$  at  $\beta_0 = 0.12$ ,  $\beta_2 = -0.11$ .

and is therefore quite strongly interacting. We estimate the overall accuracy of our bound as  $\pm 60 \text{ GeV}$ . This includes the statistical error and systematic uncertainty of the measurements of  $M_H$  (see section 3.4) as well as the systematic uncertainty assigned to fine tuning. The latter should also allow for effects of the hereto neglected  $b_2$  coupling in eq. (2.1.1). The meaning of the error is that it would be quite surprising if evidence were produced for a reasonable generic model of the scalar sector with observable cutoff effects bound by a few percent, but a Higgs mass larger than  $770 \text{ GeV}$ . It would be even more surprising if a future analysis ended up concluding that the bound is some number less than  $650 \text{ GeV}$ .

The first estimates for the nearest-neighbor hypercubic actions gave a bound of  $640 \text{ GeV}$  [3,4] which is about 10% below the new number whereas the old  $F_4$  bound was  $590 \text{ GeV}$  [5]. Thus, the older results have proven to be quite robust and this is an indication that more search in the space of actions is unlikely to yield surprises.



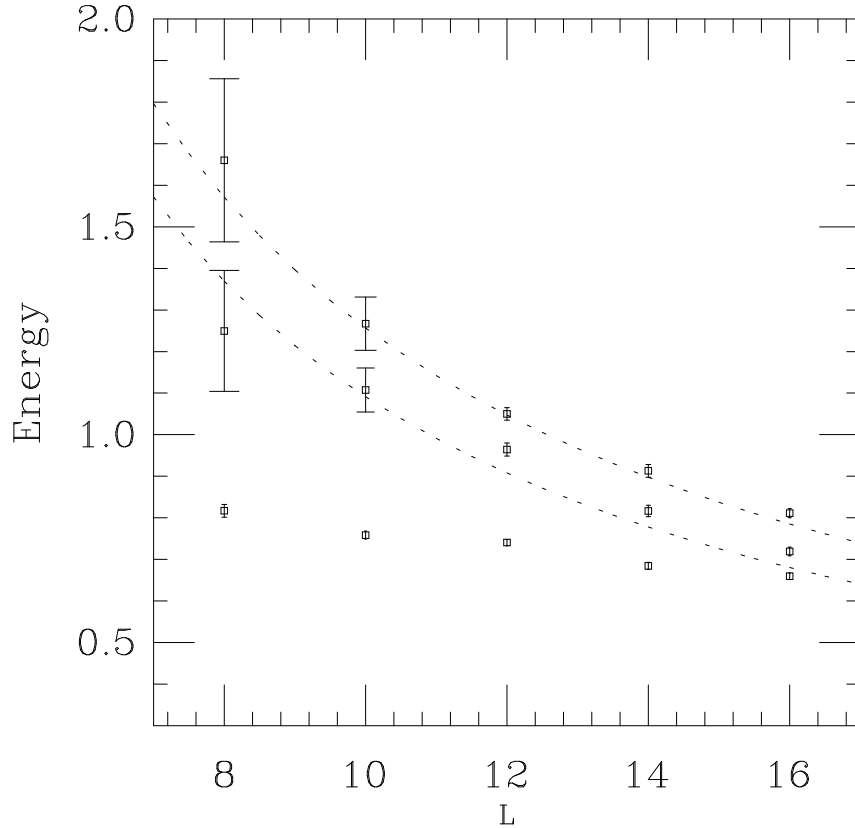


**Figure 3.6** Same as Figure 3.4 but for action  $S_3$  at  $\beta_0 = 0.1175$ ,  $\beta_2 = -0.11$ .

#### ACKNOWLEDGMENTS.

The simulations for obtaining the phase diagram and measurements on some of the smaller lattices were done on the cluster of IBM workstations at SCRI. The other measurements were done on the CRAY Y-MP at FSU. This research was supported in part by the DOE under grant # DE-FG05-85ER250000 (UMH, MK and PV), grant # DE-FG05-92ER40742 (UMH and PV), and under grant # DE-FG05-90ER40559 (HN).

## APPENDIX A.

For the interested reader we sketch in this appendix the large  $N$  analysis for action  $S'_3$  that was not treated in [9]. We can write the action  $S'_3$  as in eq. (5.1) of [9]

$$S'_3 = \eta N(\beta_0 + \beta_2) \frac{1}{2} \int_{x,y} \vec{\Phi}(x) g_{x,y} \vec{\Phi}(y) - N\beta_2 \frac{\eta^2}{8\epsilon} \int_x \left[ \int_y \vec{\Phi}(x) g_{x,y} \vec{\Phi}(y) \right]^2 \quad (\text{A.1})$$

with

$$\begin{aligned} \eta &= 6, \quad \epsilon = 18, \quad \int_x = 2 \sum_x, \quad \int_p = \int_{B^*} \frac{d^4 p}{(2\pi)^4} \\ g_{x,y} &= 6\tilde{\delta}_{x,y} - \frac{1}{3} \sum_{x' \text{ n.n. to } x} \tilde{\delta}_{y,x'} + \frac{1}{12} \sum_{x'' \text{ n.n.n. to } x} \tilde{\delta}_{y,x''} \\ g(p) &= \frac{1}{3} \sum_{\mu \neq \nu} [2 - \cos(p_\mu + p_\nu) - \cos(p_\mu - p_\nu)] \\ &\quad - \frac{1}{12} \left\{ \sum_{\mu} [2 - 2 \cos(2p_\mu)] + \sum_{\{\epsilon_\mu = \pm 1\}} \left[ 1 - \cos \left( \sum_{\mu} \epsilon_\mu p_\mu \right) \right] \right\} \\ &= p^2 + O(p^6) . \end{aligned} \quad (\text{A.2})$$

Here we used  $\tilde{\delta}_{x,y} = 1/2\delta_{x,y}$  for an  $F_4$  lattice and  $B^*$  is its Brillouin zone.

With the above notations the computations of the phase diagram, Higgs mass and cutoff effects are just as in sections 5 and 6 of [9]. We only need a few numerical constants. They are defined in [9] and for the present case take the values

$$\begin{aligned} r_0 &= 0.09932603 \\ c_1 &= 0.0281844, \quad c_2 = 2.2639 \cdot 10^{-4} \\ \gamma &= 0.01089861 \\ \zeta &= 0 . \end{aligned} \quad (\text{A.3})$$

The resulting large  $N$  plots for the Higgs mass and cutoff effects, analogous to those in [9] for the actions considered there, are shown in Figure A.1.

## APPENDIX B.

In this appendix we collect the numbers obtained from our simulations in several tables matching the graphs shown in the main text.

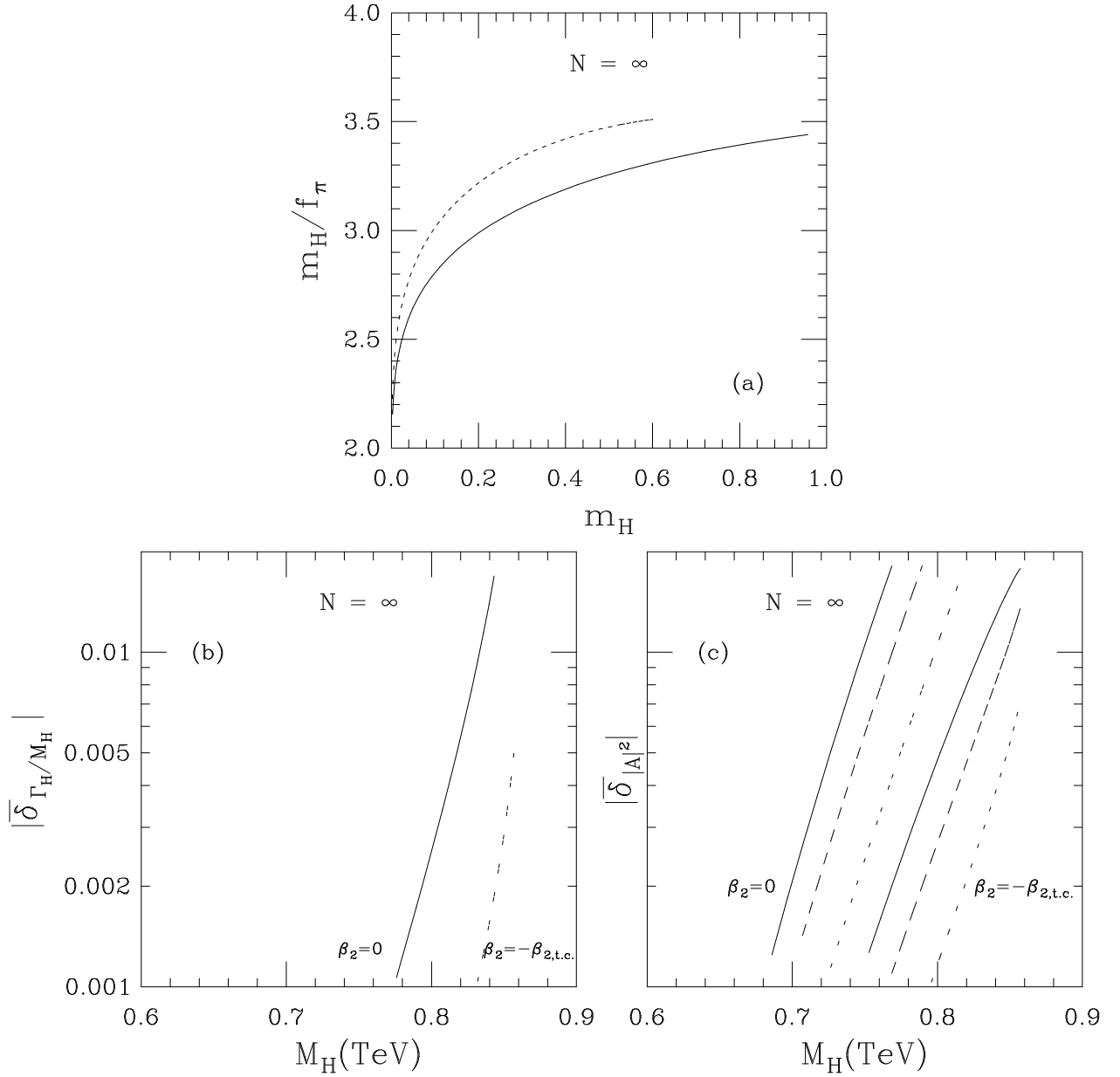


**Figure A.1** (a)  $m_H/f_\pi$  vs.  $m_H$ : The solid line corresponds to  $\beta_2 = 0$  and the dotted line to the optimal value  $\beta_2 = -\beta_{2,t.c.}$ . (b) Leading order cutoff effect in the width to mass ratio. (c) Leading order cutoff effects in the invariant  $\pi - \pi$  scattering amplitude at  $90^\circ$ . Here the dotted line represents center of mass energy  $W = 2M_H$ , the dashed line  $W = 3M_H$  and the solid line  $W = 4M_H$ .

$\beta_2$	$\beta_{0c}$
0.000	0.0917( 2)
-0.040	0.0995( 5)
-0.080	0.1070(10)
-0.110	0.1118( 3)

**Table 1** Some points of the critical line for action  $S_2$ .

$\beta_2$	$\beta_{0c}$
0.000	0.0653(3)
-0.040	0.0825(5)
-0.080	0.0990(4)
-0.110	0.1113(2)

**Table 2** Some points of the critical line for action  $S_3$ .

$\beta_0$	$m_H$	$M_H$ (GeV)
0.0925	0.198(37)	438(84)
0.0950	0.414(25)	524(32)
0.0975	0.550(27)	546(27)
0.1000	0.702(30)	593(25)
0.1050	0.830(41)	576(30)
0.1100	0.946(50)	568(30)

**Table 3** The Higgs mass  $m_H$  in lattice units and the Higgs mass  $M_H = \frac{m_H}{f} \times 246$  GeV in physical units from the numerical simulations of action  $S_1$ . The errors quoted are statistical errors only.

$\beta_0$	$m_H$	$M_H$ (GeV)
0.1120	0.126(15)	529(62)
0.1130	0.239(13)	571(30)
0.1150	0.391( 8)	627(12)
0.1175	0.534( 8)	672(10)
0.1200	0.646( 9)	696(10)
0.1225	0.721(10)	694(10)

**Table 4** Same as in Table 3 but for the action  $S_2$  at  $\beta_2 = -0.11$ .

$\beta_0$	$m_H$	$M_H$ (GeV)
0.1125	0.302( 7)	634(15)
0.1150	0.528(12)	699(16)
0.1175	0.663(11)	708(12)

**Table 5** Same as in Table 3 but for the action  $S_3$  at  $\beta_2 = -0.11$ .

L	Three lowest energy levels			Two lowest free $\pi - \pi$	
8	0.802(24)	1.202(54)	1.818(77)	1.362	1.571
10	0.801(25)	1.005(47)	1.315(67)	1.089	1.257
12	0.754(13)	0.894(18)	1.063(19)	0.907	1.047
14	0.739(16)	0.804(23)	0.916(27)	0.777	0.898
16	0.721(33)	0.679(23)	0.839(23)	0.680	0.785

**Table 6** The low lying spectrum for action  $S_1$  for various lattice sizes as measured in a numerical simulation at  $\beta_0 = 0.10$ . The two lowest energy levels of a free two pion state of zero total three-momentum are also given.

L	Three lowest energy levels			Two lowest free $\pi - \pi$	
8	0.792(24)	1.277(102)	1.711(223)	1.362	1.571
10	0.775(14)	1.115( 36)	1.171( 39)	1.089	1.257
12	0.686(16)	0.889( 32)	1.034( 38)	0.907	1.047
14	0.673(15)	0.794( 24)	0.914( 25)	0.777	0.898
16	0.656(20)	0.728( 21)	0.863( 27)	0.680	0.785

**Table 7** Same as in Table 6 but for action  $S_2$  at  $\beta_0 = 0.12$ ,  $\beta_2 = -0.11$ .

L	Three lowest energy levels			Two lowest free $\pi - \pi$	
8	0.817(15)	1.250(146)	1.660(196)	1.369	1.571
10	0.759( 9)	1.108( 53)	1.267( 64)	1.091	1.257
12	0.740( 8)	0.964( 16)	1.050( 15)	0.908	1.047
14	0.684( 8)	0.817( 14)	0.913( 15)	0.778	0.898
16	0.659( 8)	0.719( 10)	0.811( 11)	0.680	0.785

**Table 8** Same as in Table 6 but for action  $S_3$  at  $\beta_0 = 0.1175$ ,  $\beta_2 = -0.11$ .

## REFERENCES

- 1) B. W. Lee, C. Quigg, H. B. Thacker, *Phys. Rev.* **D16** (1977) 1519.
- 2) N. Cabbibo, L. Maiani, G. Parisi, R. Petronzio, *Nucl. Phys.* **B158** (1979) 295;  
B. Freedman, P. Smolensky, D. Weingarten, *Phys. Lett.* **113B** (1982) 209; R.

- Dashen and H. Neuberger, *Phys. Rev. Lett.* **50** (1983) 1897; H. Neuberger, *Phys. Lett.* **B199** (1987) 536.
- 3) M. Lüscher and P. Weisz, *Nucl. Phys.* **B318** (1989) 705.
  - 4) J. Kuti, L. Lin and Y. Shen, *Phys. Rev. Lett.* **61** (1988) 678; A. Hasenfratz, K. Jansen, J. Jersak, C. B. Lang, T. Neuhaus, H. Yoneyama *Nucl. Phys.* **B317** (1989) 81; G. Bhanot, K. Bitar, *Phys. Rev. Lett.* **61** (1988) 798; U. M. Heller, H. Neuberger and P. Vranas *Phys. Lett.* **B283** (1992) 335; U. M. Heller, M. Klomfass, H. Neuberger and P. Vranas, *Nucl. Phys. B (Proc. Suppl)* **26** (1992) 522.
  - 5) G. Bhanot, K. Bitar, U. M. Heller and H. Neuberger, *Nucl. Phys.* **B353** (1991) 551 (*Erratum Nucl. Phys.* **B375** (1992) 503).
  - 6) M. Göckeler, H. A. Kastrup, T. Neuhaus and F. Zimmermann, preprint HLRZ 92–35/PITHA 92-21.
  - 7) “The Standard Model Higgs Boson”, **Vol. 8**, *Current Physics Sources and Comments*, edited by M. B. Einhorn, North Holland, 1991.
  - 8) H. Neuberger, U. M. Heller, M. Klomfass, P. Vranas, Talk delivered at the XXVI International Conference on High Energy Physics, August 6-12, 1992, Dallas, TX, USA; FSU–SCRI–92C–114, to appear in the proceedings.
  - 9) U. M. Heller, H. Neuberger, P. Vranas, FSU–SCRI–92–99/RU–92–18, to appear in *Nucl. Phys. B*.
  - 10) M. Lüscher, *Nucl. Phys.* **B354** (1991) 531; *Nucl. Phys.* **B364** (1991) 237.
  - 11) F. Zimmermann, J. Westphalen, M. Göckeler, H. A. Kastrup, talk presented by F. Z. at the International Symposium Lattice '92, Amsterdam, Sept. 15–19, 1992; to appear in the proceedings.
  - 12) U. M. Heller, M. Klomfass, H. Neuberger and P. Vranas, FSU–SCRI–92C–150/RU–92–43, to appear in the proceedings of the *LATTICE '92* conference in Amsterdam.
  - 13) A.M. Ferrenberg and R.H. Swendsen, *Phys. Rev. Lett.* **61** (1988) 2635, [erratum 63, (1989), 1658]; *Phys. Rev. Lett.* **63** (1989) 1196.
  - 14) U. M. Heller, H. Neuberger, *Phys. Lett.* **207B** (1988) 189; H. Neuberger, *Phys. Rev. Lett.* **60** (1988) 889.
  - 15) M. Klomfass, to appear in the proceedings of the *LATTICE '92* conference in Amsterdam, and in preparation. See also Ph.D. thesis, FSU–SCRI–92T-117 (1992).
  - 16) M. Lüscher, U. Wolff, *Nucl. Phys.* **B339** (1990) 222.